

# Mass enhancement in multiple bands approaching optimal doping in a high-temperature superconductor.

C.M. Moir,<sup>1,2</sup> Scott C. Riggs,<sup>2</sup> J.A. Galvis,<sup>2</sup> Jiun-Haw Chu,<sup>3</sup> P.  
Walmsley,<sup>4</sup> Ian R. Fisher,<sup>4,5</sup> A. Shekhter,<sup>2</sup> and G.S. Boebinger<sup>1,2</sup>

<sup>1</sup>*Florida State University, Tallahassee, FL 32306, USA*

<sup>2</sup>*National High Magnetic Field Laboratory,  
Florida State University, Tallahassee, FL 32310, USA*

<sup>3</sup>*University of Washington, Seattle, WA 98195, USA*

<sup>4</sup>*Stanford University, Stanford, CA 94305, USA*

<sup>5</sup>*SLAC National Accelerator Laboratory, Menlo Park, CA 94025, USA*

(Dated: August 29, 2016)

Pnictides provide an opportunity to study the effects of quantum criticality in a multi-band high temperature superconductor. Quasiparticle mass divergence near optimal doping, observed in two major classes of high-temperature superconductors, pnictides and cuprates [1–4], is a direct experimental indicator of enhanced electronic interactions that accompany quantum criticality. Whether quasiparticles on all Fermi surface pockets in  $\text{BaFe}_2(\text{As}_{1-x}\text{P}_x)_2$  are affected by quantum criticality is an open question, which specific heat measurements at high magnetic fields can directly address. Here we report specific heat measurements up to 35T in  $\text{BaFe}_2(\text{As}_{1-x}\text{P}_x)_2$  over a broad doping range,  $0.44 \leq x \leq 0.6$ . We observe saturation of  $C/T$  in the normal state at all dopings where superconductivity is fully suppressed. Our measurements demonstrate that quasiparticle mass increases towards optimal doping in multiple pockets, some of which exhibit even stronger mass enhancement than previously reported from quantum oscillations of a single pocket [2–6].

The divergence of quasiparticle mass near optimal doping is a direct experimental indicator of enhanced electronic interactions, which accompany quantum criticality in high-temperature superconductors.[1–4] Indeed, the mass divergence deduced from quantum os-

cillation measurements at high magnetic fields up to 90T provides direct evidence for a quantum critical point at critical doping in  $\text{YBa}_2\text{Cu}_3\text{O}_\delta$  [1]. Mass divergence has also been reported in quantum oscillations studies of a high-temperature pnictide superconductor,  $\text{BaFe}_2(\text{As}_{1-x}\text{P}_x)_2$  [2–4] which, coupled with with elastoresistivity measurements in  $\text{BaFe}_2(\text{As}_{1-x}\text{P}_x)_2$ , and elastic moduli and specific heat studies of  $\text{Ba}(\text{Fe}_{1-x}\text{Co}_x)\text{As}_2$  [7–10], support the picture that the physics underlying all high temperature superconductor phase diagrams are driven by quantum criticality. Pnictides provide an exciting opportunity to study the effects of quantum criticality in a system with multiple pockets distributed throughout the Brillouin zone.

Quantum oscillation studies of  $\text{BaFe}_2(\text{As}_{1-x}\text{P}_x)_2$  to date are only able to resolve the evolution of mass over a broad range of doping for a single pocket [2–4]. Specific heat determines the sum of the masses of all Fermi pockets and thereby can determine the evolution of the total mass of all Fermi surface pockets as one approaches optimal doping. In this study, we utilize high magnetic fields to suppress superconductivity and reveal the doping dependence of the sum of quasiparticle masses through the measurement of the specific heat, and by extension electronic density of states at the Fermi surface in the normal state.

The measurement of specific heat up to magnetic fields as high as 35T provides direct information about the normal state and the nodal structure of the superconducting gap. Assuming the validity of BCS phenomenology in high-temperature superconductors, the jump in specific heat at the superconducting transition temperature,  $T_c$ , has been previously used to deduce the density of states in the normal state, and to probe the enhancement of the effective mass at  $T_c$  [2, 7, 9–14]. However, since there is no solid evidence of the validity of BCS phenomenology in unconventional superconductors, such as  $\text{BaFe}_2(\text{As}_{1-x}\text{P}_x)_2$ , it is desired to explore a different way to determine the normal state density [15, 16]. The specific heat measurements at low temperatures as a function of magnetic field presented in this work provide a model-independent determination of the doping evolution of the total mass of all electron quasiparticles near a quantum critical point in a multi-band superconductor.

Figure 1a shows the magnetic field dependence of specific heat divided by temperature,  $C/T$ , of  $\text{BaFe}_2(\text{As}_{1-x}\text{P}_x)_2$  for  $x = 0.46$  ( $T_c = 19.5\text{K}$ ) at 1.5K. Two striking features are apparent:  $\sqrt{H}$  behavior at low magnetic fields, followed by saturation above a field we denote

$H_{\text{sat}}$ . In a normal metallic state, one expects no field dependence of  $C/T$ . Therefore, we interpret the value of  $C/T$  above  $H_{\text{sat}}$ ,  $(C/T)_{\text{sat}}$ , as the specific heat of  $\text{BaFe}_2(\text{As}_{1-x}\text{P}_x)_2$  in the normal state where superconductivity is fully suppressed (See SI) [16, 17]. The  $\sqrt{H}$  behavior of  $C/T$  is a hallmark of a nodal superconducting gap, for which independent evidence exists in  $\text{BaFe}_2(\text{As}_{1-x}\text{P}_x)_2$  [18–26]. Note that the slope of the  $\sqrt{H}$  behavior increases slightly with increasing temperature (Figure 1b) and that at finite temperature the  $\sqrt{H}$  behavior does not extend to very low fields. Instead, at very low fields  $C/T$  exhibits field dependence much weaker than  $\sqrt{H}$ . Both of these observations are consistent with the Volovik phenomenology, which requires a monotonic increase of the slope of  $\sqrt{H}$  with increasing temperature and  $C/T \propto H$  at very low fields (see SI) [24–26]. Importantly, within Volovik phenomenology the low-field deviation from  $\sqrt{H}$  behavior must disappear in the zero-temperature limit because it originates from the excitation of quasiparticles across the superconducting gap at finite temperature near the gap nodes [24–26].

In Figure 1b, we extrapolate the  $\sqrt{H}$  dependence to zero field and define  $(C/T)_{\text{extrap}}$  as the value of  $C/T$  at the intercept. We then define  $\gamma_H = (C/T)_{\text{sat}} - (C/T)_{\text{extrap}}$ , which is temperature-independent for sufficiently low temperatures as shown in Figure 1b.  $\gamma_H$  represents the electronic specific heat recovered by suppressing superconductivity: it is the component of  $C/T$  directly associated with quasiparticles on Fermi surface pockets that superconduct, because all other contributions, including phonons, are magnetic-field-independent at low temperatures, as discussed above. In Figure 1c, we determine  $\gamma_{\text{bg}}$ , the background electronic  $C/T$  at zero-field and zero-temperature, by extrapolating  $C/T$  to zero temperature.

Using the physical picture discussed in connection with Figure 1 as a blueprint, we examine the behavior of the electronic specific heat for several chemical compositions in the range  $x = 0.44$  to  $x = 0.6$  (as color-coded in Figure 2a). All exhibit both  $\sqrt{H}$  dependence at low field and saturation behavior at high field (Figure 2b). We can read the value of  $\gamma_H$  directly from the panels of Figure 2b corresponding to each doping. The value of  $\gamma_{\text{bg}}$  can also be directly read from the plots of  $C/T$  versus  $T^2$  at zero magnetic field for each doping (Figure 2c,e). Note that both  $\gamma_H$  and  $\gamma_{\text{bg}}$  show strong, but opposite, doping-dependences on doping (Figure 2d,e).

The doping dependence of  $\gamma_H$  is shown in Figure 3. Clear enhancement of the total quasiparticle density of states on the Fermi surface is observed approaching optimal doping in the  $0.44 \leq x \leq 0.6$  doping range. This observation is an independent evidence for the enhancement of electron-electron interactions that are responsible for quasiparticle mass increase near a quantum critical point. The doping evolution of the Fermi surface density of states can be compared with mass enhancement as determined by quantum oscillation measurements, which is an independent indicator of enhanced interactions in the critical region[2–6]. To convert the density of states on the Fermi surface to an equivalent quasiparticle mass we will use the expression for an effective 2D (cylinder-shaped) Fermi surface,  $\gamma = 1.5 \sum_i m_i$ , where the factor 1.5 depends upon the unit cell size, atomic mass per formula unit and warping (SI).

Figure 3 also shows that the equivalent mass associated with our  $\gamma_H$  (blue circles) is enhanced by about 110%, whereas the mass determined by quantum oscillation measurements (open black squares) over the same doping range increases by only about 40% for a single electron pocket (denoted the  $\beta$  pocket) [2, 3]. The equivalent mass associated with  $\gamma_H$  inherently accounts for all pockets that open a superconducting gap below the superconducting temperature, whereas the quantum oscillations in overdoped  $\text{BaFe}_2(\text{As}_{1-x}\text{P}_x)_2$  only determine doping evolution of the mass of a single electron pocket ( $\beta$ ) [2, 3]. It is plausible that pockets for which a quantum oscillation mass is not resolved by these measurements over a broad doping range have stronger mass enhancement, thus accounting for this difference. Our data therefore suggest that some pockets must have an even stronger mass enhancement than that reported for the  $\beta$  pocket.

Further information can be obtained by considering the absolute value of  $\gamma_H$ . The total mass of all pockets from quantum oscillation measurements at  $x = 0.63$  (triangle) [6] and in the parent compound ( $x = 1$ ) (arrow) [5] are also shown in Figure 3. Both are higher than the total quasiparticle mass deduced from  $\gamma_H$ , even at our highest doping,  $x = 0.6$ . Rather than considering non-monotonic doping dependence of the total mass, we note that  $\gamma_{\text{total}} = \gamma_H + \gamma_{\text{bg}}$  (red circles) matches better the quantum oscillation data available for the total mass of all pockets. This suggests that  $\gamma_{\text{total}}$ , not  $\gamma_H$ , corresponds to the Fermi surface density of states of all pockets. Such interpretation implies that  $\gamma_{\text{bg}}$  corresponds

to the density of states of a non-superconducting pocket or pockets. Since  $\gamma_{\text{bg}}$  decreases approaching optimal doping, such a non-superconducting pocket would experience a mass decrease by a factor two in the same doping range over which the superconducting pockets double their mass. However, ARPES measurements report comparable superconducting gap energies for all pockets [18]. The observed doping dependence of  $\gamma_{\text{bg}}$  might alternatively suggest a non-Fermi surface origin of that component of the specific heat, arising perhaps from localized electrons. Another possibility is that  $\gamma_{\text{bg}}$  arises from non-Fermionic modes associated with quantum criticality [27, 28]. We emphasize that these questions can now be discussed based on a model-independent analysis of magnetic-field-dependent specific heat as presented in this work. Aside from discussion of whether all pockets superconduct at low temperature, our measurements demonstrate unambiguously that quasiparticle mass increases towards optimal doping, and that some pockets must have even stronger mass enhancement than the  $\beta$ -pocket discussed in quantum oscillation studies.

**Acknowledgments.** The work at the National High Magnetic Field Laboratory is supported by National Science Foundation Cooperative Agreement No. DMR-1157490 and the State of Florida.

- 
- [1] Ramshaw, B. *et al.* Quasiparticle mass enhancement approaching optimal doping in a high- $T_c$  superconductor *Science* **348**, 317-320 (2015).
  - [2] Walmsley, P. *et al.* Quasiparticle mass enhancement close to the Quantum Critical Point *PRL* **110**, 257002 (2013).
  - [3] Shishido, H. *et al.* Evolution of the Fermi surface of  $\text{BaFe}_2(\text{As}_{1-x}\text{P}_x)_2$  on entering the superconducting dome *PRL* **104**, 057008 (2010).
  - [4] Carrington, A. Quantum oscillation studies of the Fermi surface of iron-pnictide superconductors *Rep. Prog. Phys.* **74**, 124507 (2011).
  - [5] Arnold, B. J. *et al.* Nesting of electron and hole Fermi surfaces in nonsuperconducting  $\text{BaFe}_2(\text{As}_{1-x}\text{P}_x)_2$  *Phys. Rev. B* **83**, 220504(R) (2011).
  - [6] Analytis, J. G. *et al.* Enhanced Fermi-surface nesting in superconducting  $\text{BaFe}_2(\text{As}_{1-x}\text{P}_x)_2$  revealed by the de Haas-van Alphen effect *PRL* **105**, 207004 (2010).

- [7] Hardy, F. *et al.* Doping evolution of superconducting gaps and electronic densities of states in  $\text{Ba}(\text{Fe}_{1-x}\text{Co}_x)\text{As}_2$  iron pnictides *EPL* **91** , 47008 (2010) .
- [8] Kuo, Hseuh-Hui. *et al.* Ubiquitous signatures of nematic quantum criticality in optimally doped Fe-based superconductors *Science* **352**, 958-962 (2016).
- [9] Bohmer, A.E. *et al.* Nematic susceptibility of hole-doped and electron-doped  $\text{BaFe}_2\text{As}_2$  iron-based superconductor from shear modulus measurements *Phys. Rev. B* **112** , 047001 (2014).
- [10] Yoshizawa, Masahito *et al.* Structural quantum criticality and superconductivity in iron-based superconductor  $\text{Ba}(\text{Fe}_{1-x}\text{Co}_x)\text{As}_2$  *J. Phys. Soc. Jpn. And J. Phys. Soc.* **81** , 024604 (2012) .
- [11] Diao, Z. *et al.* Microscopic parameters from high-resolution specific heat measurements on superoptimally substituted  $\text{BaFe}_2(\text{As}_{1-x}\text{P}_x)_2$  single crystals *Phys. Rev. B* **93**, 014509 (2016).
- [12] Campanini, A. *et al.* Quantum oscillation studies of the Fermi surface of iron-pnictide superconductors *Rep. Prog. Phys.* **91**, 245142 (2015).
- [13] Chaparro, C. *et al.* Doping dependence of the specific heat of single-crystal  $\text{BaFe}_2(\text{As}_{1-x}\text{P}_x)_2$  *Phys. Rev. B* **85**, 184525 (2012).
- [14] Diao, Z. *et al.* Microscopic parameters from high-resolution specific heat measurements on superoptimally substituted  $\text{BaFe}_2(\text{As}_{1-x}\text{P}_x)_2$  single crystals *Phys. Rev. B* **93**, 014509 (2016).
- [15] Zaanen, J. Specific-heat jump at the superconducting transition and the quantum critical nature of the normal state of pnictide superconductors *Phys. Rev. B* **80**, 212502 (2009).
- [16] Analytis, J. G. *et al.* Transport near a quantum critical point in  $\text{BaFe}_2(\text{As}_{1-x}\text{P}_x)_2$  *Nature Physics* **10**, 194-197 (2014).
- [17] Putzke, C. *et al.* Anomalous critical fields in quantum critical superconductors *Nat. Commun.* **5** , 5679 (2014) .
- [18] Zhang, Y. *et al.* Nodal superconducting-gap structure in ferropnictide superconductor  $\text{BaFe}_2(\text{As}_{0.7}\text{P}_{0.3})_2$  *Nature Physics* **8**, 371375 (2012).
- [19] Hashimoto, K. *et al.* Line nodes in the energy of superconducting  $\text{BaFe}_2(\text{As}_{1-x}\text{P}_x)_2$  single crystals as seen via penetration depth and thermal conductivity *Phys. Rev. B* **81**, 220501(R) (2010).
- [20] Malone, L. *et al.* Superconducting gap structure of  $\text{BaFe}_2(\text{As}_{1-x}\text{P}_x)_2$  arXiv:1409.7523.
- [21] Reid, J-Ph. Nodes in the gap structure of the iron arsenide superconductor  $\text{Ba}(\text{Fe}_{1-x}\text{Co}_x)\text{As}_2$  from c-axis heat transport measurements *Phys. Rev. B.* **82**, 064501 (2010).
- [22] Tanatar, M.A. *et al.* Doping dependence of heat transport in the iron-arsenide superconductor

- Ba(Fe<sub>1-x</sub>Co<sub>x</sub>)As<sub>2</sub> : from isotropic to a strongly k-dependent structure *PRL* **104**, 067002 (2010).
- [23] Murphy, J. *et al.* Angular-dependent upper critical field of overdoped Ba(Fe<sub>1-x</sub>Ni<sub>x</sub>)As<sub>2</sub> *Phys. Rev. B* **87**, 094505 (2013).
- [24] Volovik, G.E. Superconductivity with lines of GAP nodes: density of states in the vortex *Pis'ma Zh. Eksp. Teor. Fiz.* **58**, 457-461 (1993).
- [25] Kopnin, N.B. and G.E. Volovik Flux Flow in d-wave superconductors: low temperature universality and scaling *Phys. Rev. Lett.* **79**, 1377 (1997).
- [26] Hussey, N.E. Low-energy quasiparticles in high-Tc cuprates *Adv. Phys.* **51**, 1685-1771 (2002).
- [27] Oganesyan, Vadim, Steven A. Kivelson, and Eduardo Fradkin Quantum theory of a nematic Fermi fluid *Phys. Rev B* **64**, 195109 (2001).
- [28] Kogan, V.G. Strong pairbreaking in anisotropic superconductors *Phys. Rev. B* **81**, 184528 (2010).
- [29] Nakajima, Masamichi *et al.* Growth of BaFe<sub>2</sub>(As<sub>1-x</sub>P<sub>x</sub>)<sub>2</sub> single crystals (0≤x≤1) by Ba<sub>2</sub>As<sub>3</sub>/Ba<sub>2</sub>P<sub>3</sub>-flux method *J. Phys. Soc. Jpn.* **81**, 104710 (2012).

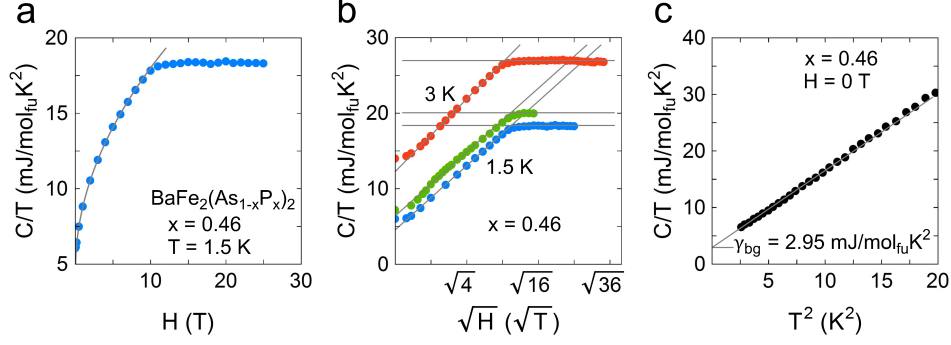


FIG. 1: **a** Field dependence of specific heat divided by temperature,  $C/T$ , of  $\text{BaFe}_2(\text{As}_{1-x}\text{P}_x)_2$  ( $T_c = 19.5\text{K}$ ) at  $T = 1.5\text{K}$ . The line indicates  $\sqrt{H}$  behavior which is consistent with phenomenology associated with a superconducting gap with nodes.[24, 25] **b** Field dependence of  $C/T$  plotted against  $\sqrt{H}$  at 1.5K (blue), 1.75K (green), and 3K (red). Solid grey lines indicate the two distinct regimes:  $\sqrt{H}$  behavior and saturation behavior. The slope of the  $\sqrt{H}$  behavior at 1.5k and 1.75K is  $4.25 \frac{\text{mJ}}{\text{molK}^2\sqrt{\text{T}}}$  and at 3K is  $4.8 \frac{\text{mJ}}{\text{molK}^2\sqrt{\text{T}}}$ . **c** Temperature dependence of  $C/T$  at zero magnetic field, where the grey line indicates the low temperature specific heat behavior:  $C/T = \gamma + \beta T^2$ , from which  $\gamma_{\text{bg}}$  is extrapolated.



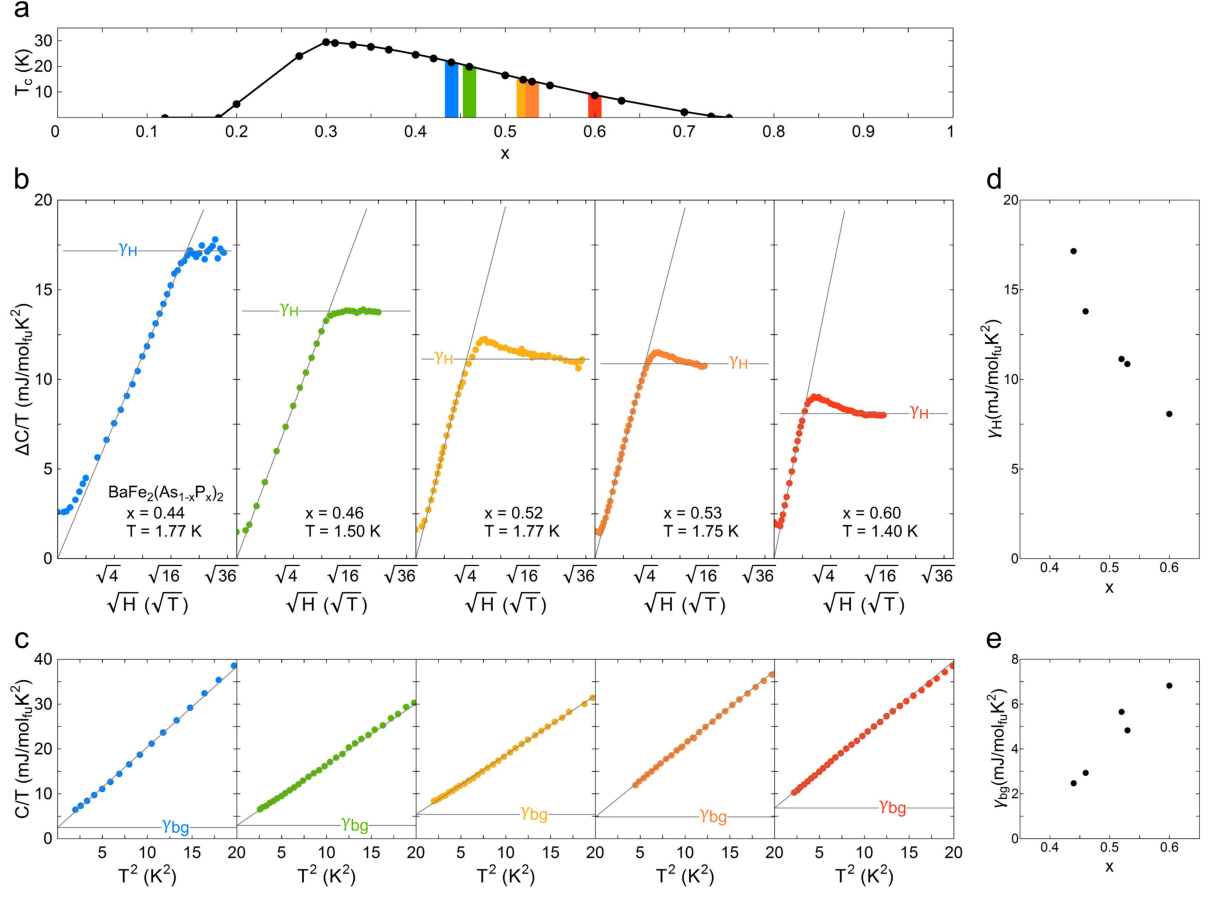


FIG. 2: **a**  $T_c$  as a function of doping for  $\text{BaFe}_2(\text{As}_{1-x}\text{P}_x)_2$  aggregated from previous studies [2, 6, 16, 29]. Colored lines indicate the doping values of samples studies in this work. **b** The change in  $C/T$ ,  $\Delta C/T = C/T(H) - (C/T)_{\text{extrap}}$  (see text), from  $\gamma_{\text{extrap}}$  (see text) of  $\text{BaFe}_2(\text{As}_{1-x}\text{P}_x)_2$  at low temperatures. Lines indicate  $\sqrt{H}$  behavior and saturation at  $\gamma_H$ , which decreases with increasing doping. **c** Zero field  $C/T$  as a function of  $T^2$  in the low temperature regime. Grey lines indicate best agreement to  $\gamma + \beta T^2$ , the extrapolation of which defines  $\gamma_{bg}$ . **d** Doping dependence of  $\gamma_H$ . **e** Doping dependence of  $\gamma_{bg}$ .

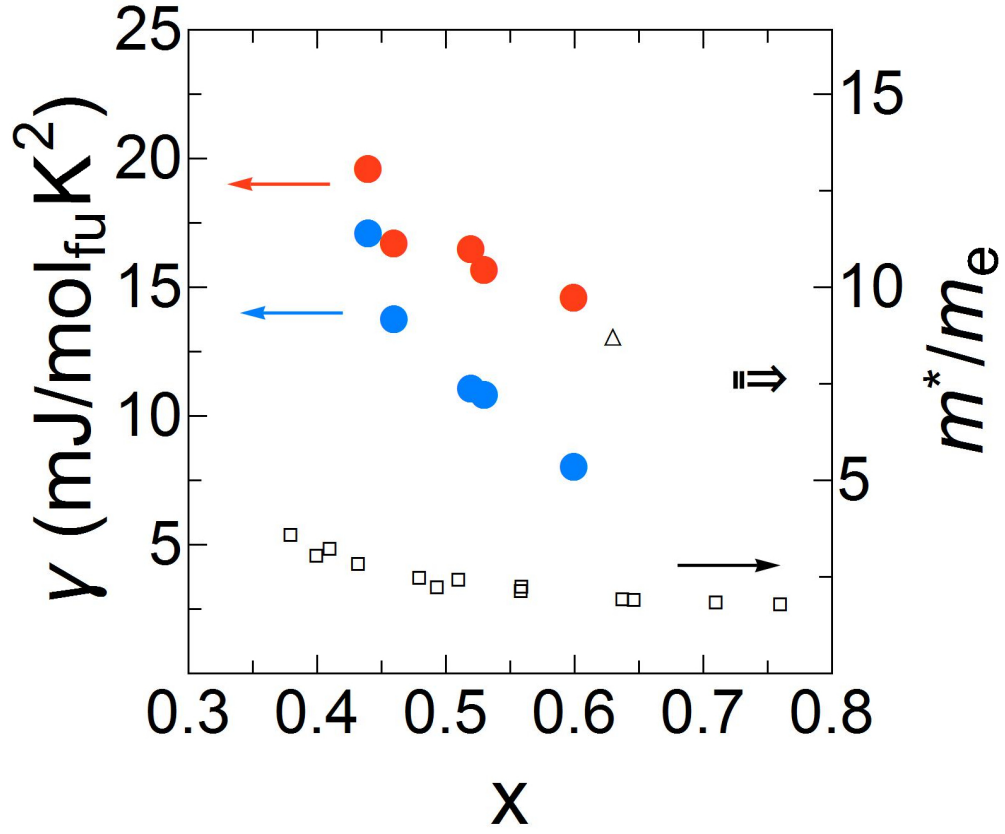


FIG. 3: Doping dependence of the quasiparticle density of states and quasiparticle masses of  $\text{BaFe}_2(\text{As}_{1-x}\text{P}_x)_2$ .  $\gamma_H$  is represented by blue circles,  $\gamma_{total}$  is represented by red circles. The empty triangle represents total mass from Ref. 6. The arrow indicates the total mass in the parent compound,  $x = 1$  [5]. Empty squares represent the beta pocket mass from Refs. 2-4.